Faraday Discussions

Accepted Manuscript

This manuscript will be presented and discussed at a forthcoming Faraday Discussion meeting. All delegates can contribute to the discussion which will be included in the final volume.

Register now to attend! Full details of all upcoming meetings: http://rsc.li/fd-upcoming-meetings

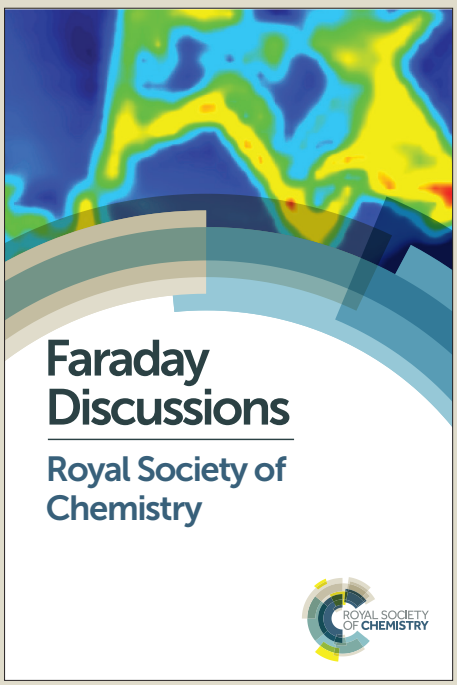

This is an *Accepted Manuscript*, which has been through the Royal Society of Chemistry peer review process and has been accepted for publication.

Accepted Manuscripts are published online shortly after acceptance, before technical editing, formatting and proof reading. Using this free service, authors can make their results available to the community, in citable form, before we publish the edited article. We will replace this *Accepted Manuscript* with the edited and formatted *Advance Article* as soon as it is available.

You can find more information about *Accepted Manuscripts* in the Information for Authors.

Please note that technical editing may introduce minor changes to the text and/or graphics, which may alter content. The journal's standard Terms & Conditions and the Ethical guidelines still apply. In no event shall the Royal Society of Chemistry be held responsible for any errors or omissions in this *Accepted Manuscript* or any consequences arising from the use of any information it contains.

ROYAL SOCIETY OF CHEMISTRY

www.rsc.org/faraday_d

3 Bisphosphonate ligands improve the water solubility of quantum dots.

Siti Fatimah Abdul Ghani[1], Michael Wright[1], Juan Gallo Paramo[2], Melanie Bottrill[2,3], Mark Green [3], Nicholas Long [2], Maya Thanou [1] *
DOI: 10.1039/b000000x [DO NOT ALTER/DELETE THIS TEXT]

Synthesised Quantum Dots (QDs) require surface modification in order to improve their aqueous dispersion and biocompatibility. Here we suggest bisphosphonate molecules as agents to modify the surface of QDs for improved water solubility and biocompatibility. QDs_TOPO (CdSe/ZnS-trioctylphosphine oxide) were synthesised following modification of the method of Bawendi *et al.* QDs surface modification is performed using a ligand exchange reaction with structurally different bisphosphonates (BIPs). The BIPs used were ethylenediphosphonate (EDP), methylenediphosphonate (MDP) and imidodiphosphonate (IDP). After ligand exchange QDs were extensively purified using centrifugation, PD-10 desalting columns and mini dialysis filters. Transmission electron microscopy (TEM) and fluorescent spectroscopy have been used to characterise QDs size and optical properties. Cell toxicity was investigated using MTT (tetrazolium salt) and glutathione assays and intracellular uptake was imaged using confocal laser scanning microscopy and assessed by Inductively Coupled Plasma Mass Spectrometry (ICP-MS). QDs_TOPO and QDs-capped with BIPs (QDs_BIPs) were successfully synthesised. TEM showed the size and morphology of the quantum dots to be 5 nm – 7 nm with spherical shape. The stabilised QDs_BIPs showed significantly improved dispersion in aqueous solutions compared to QDs_TOPO. The cytotoxicity studies showed very rapid cell death for cells treated by QDs_TOPO and a minor effect on cell viability when QDs_BIPs were applied on cells. Both EDP and MDP modified quantum dots did not increase significantly the intracellular levels of glutathione. In contrast, IDP modified quantum dots increased substantially the intracellular glutathione levels indicating potential cadmium leakage and inability of IDP to cap adequately and stabilise the QDs. EDP and MDP modified QDs were taken up by IGROV-1 (ovarian cancer) cells as shown by fluorescence microscopy, however the IDP modified quantum dots signal was not clearly visible in the cells. Cellular uptake measured by intracellular cadmium levels using ICP-MS showed significant uptake of all three BIPs QDs. The structure of BIPs appears to play a significant role on the ability of these molecules to act as capping agents. Our findings demonstrate a novel approach in producing water dispersible QDs through ligand exchange with certain type of BIPs molecules that can find application in bioimaging.

1 Introduction

Semiconductor quantum dots (QDs) are nanometer-sized crystals that have unique photochemical and photophysical properties [1]. QDs are fluorescent labels that are

resistant against photobleaching, with improved brightness, size-dependant fluorescence and a narrow, tunable emission spectrum. QDs can provide the possibility of continuous, real-time imaging of single molecules and single cells over an extended period of time [2]. They exhibit narrow emission and wide excitation spectra; in fact QDs can be excited at any wavelength below their emission peak [3].Surface, core and shell composition of semiconductor QDs nanocrystals have played significant roles via their structural and optical properties; from the high surface-to-volume ratios for efficient absorption and emission spectra towards capping with higher band-gap shells consisting of either ZnS or ZnSe for improved luminescence, stability, aggregation and also toxicity [4-6].

Common QDs preparation uses a high-temperature solvent mixture of triphenylphosphine/triphenylphosphine oxide (TOP/TOPO) route yielding hydrophobic not aqueous dispersible QDs. Attempts to overcome their hydrophobicity have focused on identifying suitable ligands for ligand exchange (TOPO/TOP) as well as recently developing new methods of synthesis [4, 5]. Hydrophobicity also directly influences the readiness of the QDs for biological applications. Therefore, the challenge in developing QDs lies in the preparation method and modification of the nanoparticles towards improved biocompatibility [7].

Any phase transfer towards aqueous or water soluble QDs will require surface bio-functionalisation or modifications with hydrophilic ligands either through ligand exchange reactions or forming a micelle through hydrophobic interaction and/or silica encapsulation [7]. Ideally, surface modification or over-coating the QDs should prevent QDs from flocculating in aqueous buffers and in storage over time, able to efficiently covert the organic soluble / hydrophobic QDs into water soluble QDs, whilst maintaining the size of the QDs and the fluorescent properties. The surface modification also affects the hydrodynamic diameter of the QDs and this may have an impact on their application as diagnostic and therapeutic agents [8]. There are several procedures for coating the surface of QDs that have been developed, such as cross-linking, use of peptides, avidin and amphiphilic molecules [9-12] . The latter is an example that uses a mixture of phospholipids and lipopolymers or hydrophilic polymers with hydrophobic side chains [12].

A less investigated method of surface modification is non-covalent conjugation which includes the interaction between biofunctionalised molecules and the metal ions (Cd, Zn) present at the QDs surface. This has been reported with the use of proteins or polypeptides with amino acid sequences that have the affinity for the metallic cations [13]. The mechanism of biomolecule adsorption results from ionic bonds between the carboxylate function (COO^-) of the ligand and Cd^{2+} or Zn^{2+}.

QDs synthesis can involve the formation of the QDs nanoparticles in the presence of stabilising ligands, independent of the solvents used. These stabilising ligands carry out a very important role to maintain the discrete, non-aggregated QDs whilst affecting the photoluminescence of the nanoparticles as well. This applies especially to the uncapped QDs, where the surface ligand is the only barrier between the electron-hole pair in the core QDs and the media or solutions [14, 15]. The stability of the attachment of the stabilising ligands is crucial in reducing the cytotoxicity of the QDs in biological systems [16, 17]. There are studies that report that uncapped QDs give high cytotoxicity compared to capped or protected QDs and also uncapped QDs have been reported to induce apoptosis due to leaching of toxic metals from the QDs or by the formation of reactive oxygen species (ROS) [18, 19]. The toxicity of uncoated cadmium-containing QDs is associated with free cadmium present in the

nanocrystals suspension or intracellularly released from absorbed QDs via surface oxidation thus suggesting that the core could degrade in biological environment [14].

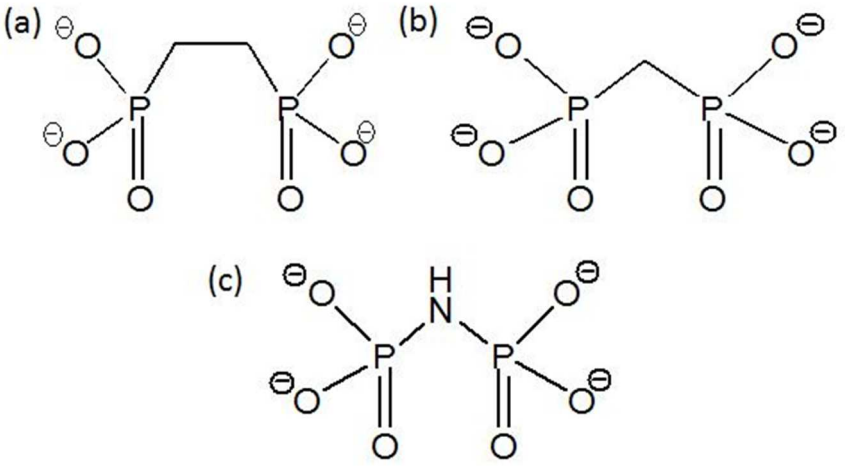

Figure 1: Structure of bisphosphonates used that mimic the pyrophosphate groups; (a) ethylene diphosphonate (EDP); (b) methylene diphosphonate (MDP); and (c) imidodiphosphonate (IDP).

Ligand exchange surface modification routes have been explored and employed with many different materials and protocols [20-22]. In the study presented here, we explore the ligand exchange route and surface modification replacing the hydrophobic surface layer (TOP/TOPO) of the QDs (core/shell CdSe/ZnS) using a hydrophilic ligand that contains phosphonate groups. We believe that this is the first approach of ligand exchange methods using this type of phosphorus containing group as the hydrophilic ligand. Bisphosphonates (BIPs) or diphosphonates feature the presence of two phosphonate groups and also mimic the structure of pyrophosphate. These two phosphonate groups are linked together by one or two central carbon atoms (C) forming the P-C-P backbone. BIPs are commonly used in treating secondary breast cancer, osteoporosis and similar diseases preventing the loss of bone mass [23]. Bisphosphonates' mechanism of action includes Ca^{2+} chelation [24]. In this study, we aim to take advantage of this property and investigate the efficiency of BIPs as QDs' capping agents. We investigate the effect of structurally similar BIPs (Figure 1) on stabilising CdSe/ZnS QDs. Ethylene diphosphonate (EDP), methylene diphosphonate (MDP) and imidodiphosphonate (IDP) are introduced on the surface of quantum dots via a designed ligand exchange reaction. The produced nanoparticles are tested for their optical properties, colloidal dispersion, and photostability as well as for their effect on cell viability and ability to label cells.

2 Experimental Materials and Methods

All materials were purchased from Sigma Aldrich Corporation, St. Louis MO, (USA); Fisher Chemicals and Loughborough (UK), and Alfa Aesar, Karlsruhe

(Germany); chemicals were of reagent grade and used as received. Schlenk-line techniques and inert gas nitrogen conditions have been used to carry out all synthetic preparations. ^{31}P-$\{^{1}H\}$ NMR analytical data were obtained using a Bruker AV 400 MHz spectrometer. All isotopic solvents d_6-DMSO, D_2O, $CDCl_3$ were purchased from Cambridge Isotope Laboratories, MA USA.

For QDs synthesis (CdSe/ZnS), materials used including trioctylphosphine oxide (TOPO, 90%), trioctylphosphine (TOP, 90%), diethylzinc ($ZnEt_2$), methylenediphosphonate (MDP) and imidodiphosphonate (IDP) were obtained from Sigma Aldrich, MO USA. Cadmium acetate dihydrates ($CdOAc_2$).$2H_2O$ and tetraethyl ethylene diphosphonate (TEDP) was purchased from Alfa Aesar. De-salting PD-10 (*Sephadex G-25 Medium)* columns were purchased from GE Life Sciences, UK. Absorption spectroscopy was recorded using a Lambda 25 UV/Vis spectrometer using 10 mm cuvette and emission spectra were obtained using a Varian Cary Eclipse Fluorescence Spectrometer or Tecan Infinite® 200 Pro. QDs were pre-scanned over the range of 400 nm - 700 nm.

Hydrodynamic diameters were measured using Nanoseries Nano-S Malvern (DLS) and were performed in quartz cuvettes prepared with at least three good quality data measurements analysed for each samples. Mass Spectrometry Analysis (LC MS/MS and ICP-MS) was obtained using a PerkinElmer SCIEX ICP-Mass Spectrometer (ELAN DRC6100, USA) at the Mass Spectrometry Facility, KCL. Transmission Electron Microscopy (TEM) and High Resolution-TEM data and images were acquired using a FEI Tecnai 12 TEM operating at 120 kV with an AMT 16000M digital camera to obtain high resolution images at the Centre for Ultrastructural Imaging (CUI), KCL. Cell imaging was carried out using A1R Si Confocal Microscopy equipped with Ti-E Inverted Microscope at the Nikon Imaging Centre, KCL.

Synthesis of BIPs capped QDs

Precursor preparation Selenium powder was added to a round bottom flask (previously purged with nitrogen) and then tri-octylphosphine (50 mL) was added carefully syringe-wise into the flask through a rubber septum. The mixture was stirred for 3 hours at room temperature to obtain a pale yellow, optically clear solution of the Se_TOP precursor. In a separate flask, sulfur powder was added to a Schlenk tube previously purged with nitrogen followed by trioctylphosphine (TOP) (5 mL) addition. The mixture was stirred overnight to make sure all the sulfur powder had dissolved completely in the TOP solvent and formed an optically clear solution to give the S_TOP precursor. A zinc and sulfur precursor solution was prepared by addition of TOP (9 mL), diethyl zinc (450 µL, 1.1 M solution in toluene) and previously prepared S-TOP (480 µL) were added into a previously nitrogen-purged Schlenk tube. The precursor mixture was left to stir for 2 - 3 hours to achieve a homogenous mixture and was freshly prepared prior to synthesis.

Synthesis of core/shell CdSe/ZnS_TOPO Tri-octylphosphine oxide (TOPO) (5.25 g) and cadmium acetate dihydrate [Cd $(CH_3COOH)_2.2H_2O$] (0.13mmol; 0.045 g) were added into a round bottom flask that was purged several times with nitrogen gas. The compound was slowly heated to 220^{o}C, stabilised at the desired temperature with moderate stirring to obtain an optically clear solution. Selenium-TOP precursor solution was injected rapidly through the rubber septum into the hot mixture. After the injection of the precursor solution, the mixture started to change colour from

pale yellow, to yellow then to orange and finally red to deep red in about 10-15 minutes. The reaction was left for 30 minutes before being cooled to 60°C. The excess TOP/TOPO was removed using methanol and centrifuged at 4000 rpm for 30 minutes to yield a fine red precipitate. In a typical synthesis, CdSe_TOPO prepared previously was added to a three necked round-bottom flask together with TOPO (3.0 g) and the mixture was heated to 190°C. The zinc and sulfur precursor was freshly prepared and introduced dropwise using a syringe. Following the final addition, the mixture was left for 30 minutes before cooling to 60°C. The nanoparticles produced were then treated three times with methanol and centrifuged at 4000 rpm for 30 minutes to yield a fine red precipitate of CdSe/ZnS_TOPO. Core and core shell quantum yields were measured to Rhodamine 6G as reference [25].

Synthesis of ethylenediphosphonate (EDP) ligand Tetraethyl ethylenediphosphonate (TEDP) was added into a round-bottom flask to equimolar hydrochloric acid (37%). The mixture was heated at reflux and left to stir overnight. A fine white powder formed overnight and was collected in a separating funnel. This was purified by washing the particles with hexane, dichloromethane and chloroform and then dried under vacuum and weighed to give 90% yield.

Data ^{31}P $\{^{1}H\}$ NMR (162 MHz, D_2O): δ 28.24 (s, P=O). ESI-MS: m/z 190 $[M^+]$. Result of HRMS 190.9874 (found)/190.9874 (calc.) m.pt.: 210°C - 215°C.

Surface modification via ligand exchange with bisphosphonates - general methodology As-prepared CdSe/ZnS_TOPO was isolated from any excess TOP/TOPO by precipitation with methanol and centrifugation at 4000 rpm for 30 minutes. The nanoparticles were then suspended in hexane in a round bottom flask; each with addition of 2 mg of either a) EDP, b) MDP; or c) IDP, followed by insertion of penta(ethylene)glycol (Penta_EG) via syringe into the mixture. The mixture was purged with nitrogen gas and left under reflux for 6 hours with vigorous stirring to ensure that the ligand exchange reactions were complete. This then yields the nanoparticles QDs_BIPs and the precipitate was dried under vacuum. The product was weighed and a yield of 80% was noted.

Purification of water soluble QDs_BIPs - general methodology An aqueous solution of QDs_BIPs (EDP/MDP/IDP) was sonicated for 5-10 minutes and passed through the PD-10 (Sephadex G-25 Medium) de-salting column. The sample was loaded until all the solution entered the packed bed material completely. The sample was eluted with purified water and the eluates were collected for further analysis. Purification steps were repeated for all QDs_BIPs (EDP/MDP/IDP) samples. BIP-modified QDs were characterised for efficient ligand exchange using ^{31}P-$\{^{1}H\}$ NMR spectroscopy.

Characterisation of QDs and QDs_BIPs

Optical measurements: Core (CdSe_TOPO) and/or core/shell (CdSe/ZnS_TOPO) were dispersed in toluene while QDs_BIPs (EDP/MDP/IDP) were dispersed in deionised water at the concentration of 1 mg mL^{-1}. Absorbance and fluorescence intensity of all solutions were obtained using a 10 mm quartz cuvette scanning from 400 nm to 700 nm in a UV/Vis spectrometer (Perkin Elmer) and fluorescence spectrometer (Varian Cary Eclipse).

Colloidal stability and photostability studies of QDs in aqueous media Purified QDs_BIPs were prepared in water, media and 10%, 20%, 50% FBS (Foetal Bovine serum) in cell culture media. All these solutions were assessed using absorbance/fluorescence measurements for photostability and colloidal stability over

4 hours. Measurements were taken using Tecan Platereader Infinite® 200 Pro Series spectrometer. Absorbance values at 550 nm wavelength were recorded for all solutions to measure the turbidity values of the solutions as an indication for QD aggregation [26].

Nanoparticle characterisation Both diluted core and core/shell (CdSe/ZnS_TOPO) in hexane and aqueous suspensions of QDs_BIPs were dropcast using a pipette onto holey carbon TEM grids (300 mesh, copper grids) horizontally placed with an inverted tweezer and left to dry for 5 minutes. Filter paper was used to passivate the solution by placing the sharp edge of the filter paper by the side of the grids. These nanoparticles were then analysed under the microscope for size and distribution. High resolution-TEM was also analysed for determination of the nanocrystals lattice spacing using FEI Tecnai G2 T20 FE TEM at a 200 Kv accelerating voltage. BIPs modified quantum dots were characterised for their ζ potential using a Malvern Nanoseries.

Energy dispersive X-ray spectroscopy (EDAX) analysis QDs_TOPO and QDs_BIPs nanoparticles were prepared in 1 mg mL^{-1} solution in hexane and in water, respectively. 5uL of these solutions were pipetted onto holey titanium grids horizontally with an inverted tweezer and left to dry under an argon lamp for 5 minutes. These nanoparticles were then analysed under the microscope for image and elemental analysis.

Cell viability assay (MTT viability assay and glutathione assay) Human ovarian adenocarcinoma cells (IGROV-1) were cultured in Roswell Park Memorial Institute (RPMI 1641) media supplemented with 2 mM glutamine, 10% v/v fetal bovine serum (FBS), 1% penicillin-streptomycin (pen-strep). Cells were cultured in a humidified atmosphere containing 5% CO_2, at 37°C. For MTT cell viability studies, the 3-(4, 5-dimethylthiazol-2-yl) - 2, 5-diphenyltetrazoliumbromide (MTT) reduction assay and glutathione assay (determination of reactive oxygen species-induced toxicity) were selected to monitor the cell viability of the proliferation of the QDs_TOPO and QDs_BIPs in media. For MTT assays, cells were seeded into 96 well plates overnight, and were then incubated with media containing QDs_TOPO and QDs_BIPs in triplicate. In each well, 10 µL of MTT reagent was added 24 hours after addition of the nanoparticles, and the plate was then incubated for 4 hours and DMSO added to each well to solubilise the formazan crystals after removing the media. Results for the MTT viability assay were expressed as:

$$\textit{Percent viability} = \frac{[\textit{Cells}_x\ \textit{(treated cells)} - \textit{background}]}{[\textit{Cells}_x\ \textit{(untreated cells)} - \textit{background}]}\ X\ 100$$

The glutathione assay was carried out to determine the reactive oxygen species-induced toxicity in cells. Total concentration of intracellular glutathione (tGSH) was determined biochemically using a Sigma glutathione assay kit. Typically, cells were counted, incubated and then lysed with the nanoparticles. Total glutathione was determined biochemically following the assay protocol by constructing the standard curve against total glutathione in each sample. It was calculated using the equation below;

Equation:

$$[\text{Total GSH}] = \left(\frac{(\text{Absorbance at 412 nm}) - (\text{y intercept})}{\text{Slope}} \right)$$

QDs_BIPs cell uptake Adherent cells (IGROV-1) were grown and counted manually using haemocytometer and seeded into an 8-well chamber plate. The chamber plate was previously primed with 10% w/v porcine skin gelatine in water overnight at 4°C. The cells were incubated for 24 hours to let them adhere to the chamber and were then dosed with RPMI media containing QDs_BIPs. Subsequently, the cells were washed with phosphate buffered saline (PBS) and fixed using 1% w/v paraformaldehyde (PFA in PBS). The cells were washed with PBS before staining them with 4', 6-diamidino-2-phenylindole (DAPI) to label the nucleus. The cells were washed again and stored in PBS before imaging with confocal laser scanning fluorescent microscopy.

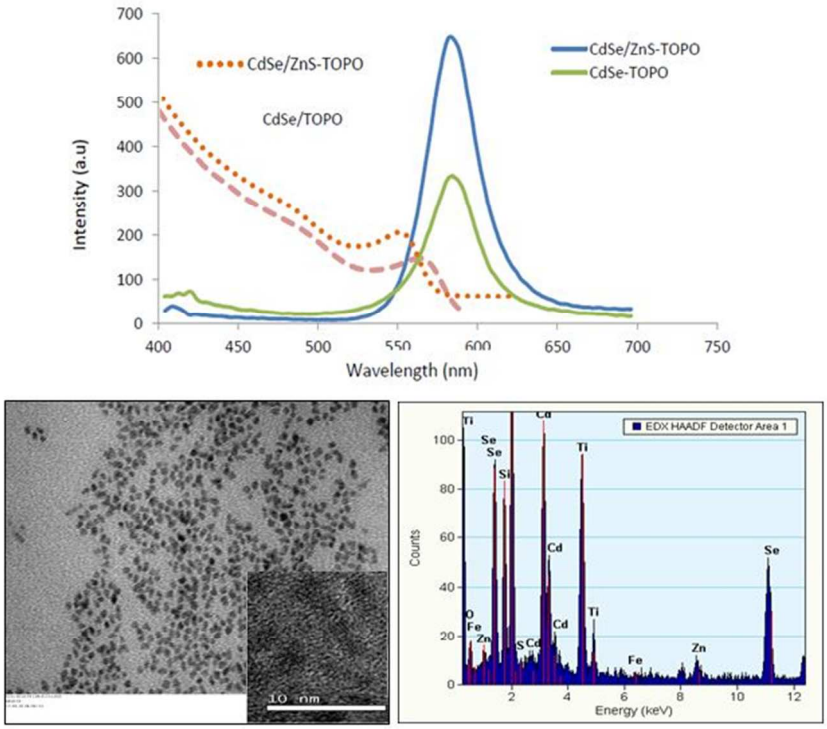

Figure 2: Characteristics of QDs core/shell CdSe/ZnS (top) absorbance and fluorescence spectrum of core CdSe in hexane; absorbance and fluorescence spectrum of core/shell CdSe/ZnS in hexane; (bottom, left) Transmission electrom microscopy (TEM) image of QDs and high resolution-TEM image (HRTEM) indicating confirmation the lattice spacing for nanocrystals, and (bottom, right) Energy Dispersive X-Ray Analysis (EDAX).

Inductively Coupled Plasma Mass Spectroscopy The levels of QDs_BIPs uptake was characterised by assessing intracellular levels of Cd^{2+} following the 24 hours incubation with the cells. QDs_TOPO (coarse dispersion in cell medium) and QDs_BIP (fine dispersion) were applied on IGROV-1 cells and were incubated for 24 hours. At the end of the experiment the supernatant was removed and cells were

washed with PBS and lysed with lysis buffer Quantification of Cd^{2+} concentration in cell uptake and in standard solution was carried out by ICP MS. Each biological sample were digested with 10 times mass or volume matter with nitric acid, HNO_3 at 60^oC overnight until all matter are digested completely. Each sample was then diluted with Mili-Q water (18.2 Ω) to give acid concentration of ~15%. Yttrium was used as internal standard and was spiked in all samples at the same concentration. Solution samples of the same used in the cellular uptake were analysed following the same procedures described above to correlate with the Cd^{2+} concentration. All samples were analysed using the same ICP MS initialisation and set up.

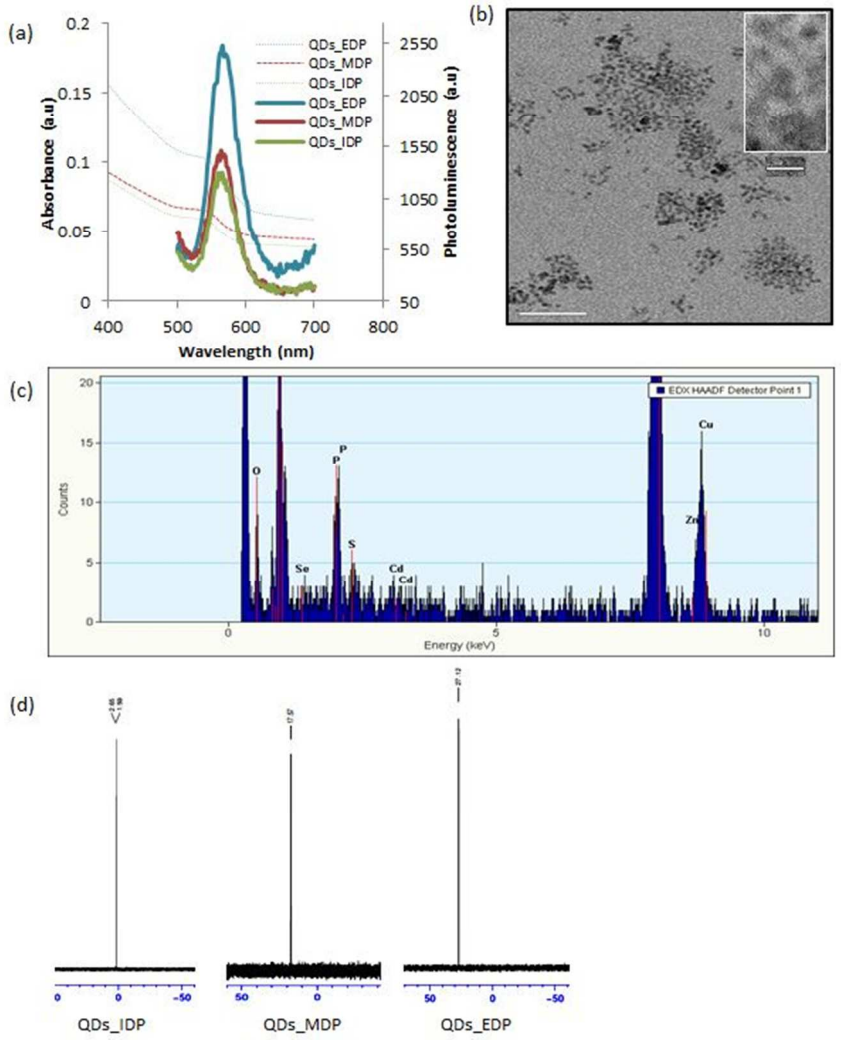

Figure 3: BIPs modified QDs, (QDs_BIPs);EDP/MDP/IDP characteristics; (a) Emission/absorbance spectra of QDs_BIPs in water at RT after the ligand exchange; (b) Transmission electron microscopy (TEM) and High Resolution TEM images of QDs_BIPs showing size and distribution in

water (scale bar:100nm, inset: 5nm); (c, d) EDAX spectra of BIPs modified QDs showed presence of elements related to BIPs_QDs; (e) ^{31}P NMR spectrum of QDs_BIPs indicating no impurities detected in the precipitate after purification (no signal recorded for TOP and TOPO). Pure TOPO in chloroform-d ^{31}P NMR shows a typical signal at ~50 ppm whilst free TOPO in chloroform-d signal at ~52 ppm.

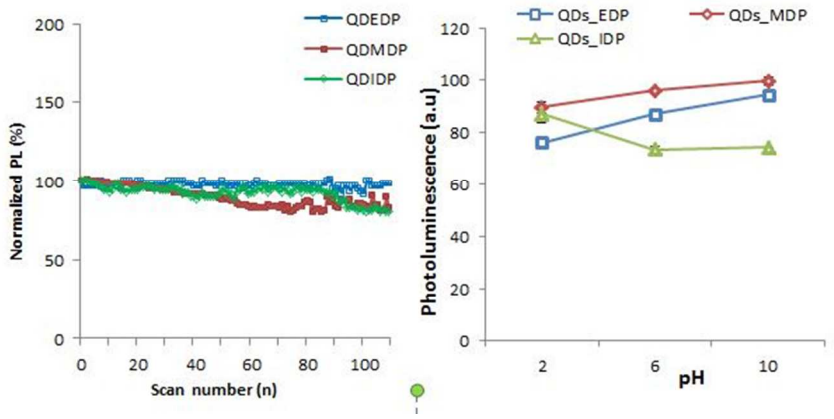

Figure 4: Photostability of aqueous dispersion of QDs_BIPs measured; (left) Photostability was measured at emission wavelength of 560nm by consecutive excitation at 365nm at room temperature. The fluorescence intensity was normalised to the initial value of photoluminescence. Finding indicate that 80% - 85% initial fluorescence intensity remain after 120 measurements/illuminations; (right) QDs_BIPs remain soluble in water under acidic to basic conditions with no decrease on photoluminescence from pH 2.0 - 10.0.

3 Results and Discussions

Core and core/shell QDs were synthesised using a modification of published procedures [27-31]. Quantum yields for both core and core/shell species were measured to be 0.17 and 0.32 respectively using Rhodamine 6G (reference QY: 0.95) as the reference fluorescence dye. The aim was to prepare colloidally stable QDs in aqueous media using the following bisphosphonates; EDP (ethylenediphosphonate), MDP (methylenediphosphonate) and IDP (imidodiphosphonate) (Figure 1). Most of the frequently used ligands for phase transfer utilise thiol or carboxylic containing capping agents [32, 33]. However, in 2004 Green *et al* reported that nucleotides such as ATP may be used as passivating agents for quantum dots[34]. Based on this report, we considered investigating bisphosphonate molecules as capping agents for water soluble quantum dots. MDP and IDP are commercially available bisphosphonates whereas EDP is prepared from tetraethylene-1, 2-diphosphonate using acidic conditions. Analysis with mass spectrometry indicated that EDP was prepared successfully (see Supplementary information). These bisphosphonates were used to modify CdSe/ZnS_TOPO quantum dots, which were selected due to their frequently reported superior optical properties. The pioneering synthesis methods of Bawendi *et al.* and Peng *et al.* [21, 44] were followed to prepare the initial quantum dots coated with TOPO to further undergo phase transfer [27, 28]. The results in Figure 2

indicate the optical characteristics of CdSe/ZnS_TOPO and CdSe_TOPO as well as size characteristics via TEM, lattice spacing via HRTEM and energy dispersive X-ray analysis. These data are in agreement with that such in previously reported studies using these methods of synthesis [30, 35].

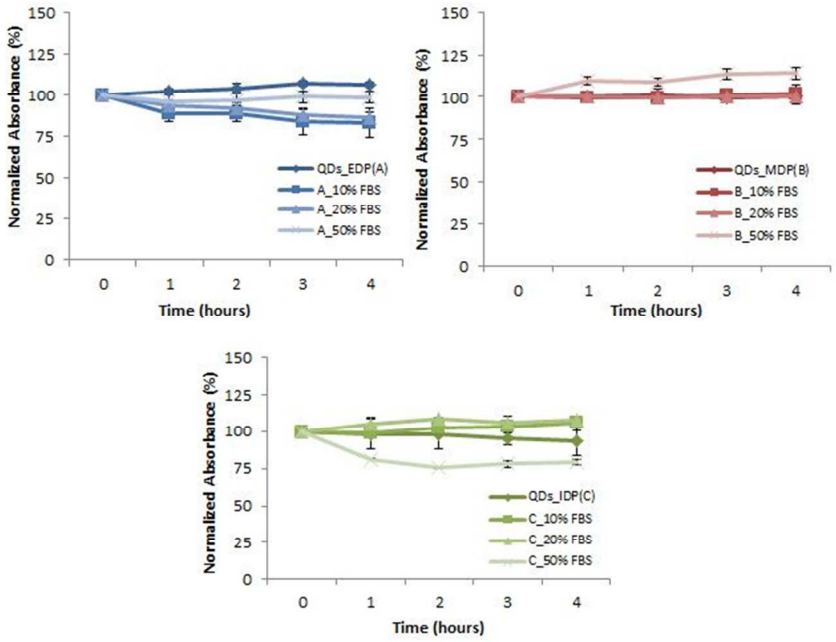

Figure 5: Stability Studies of QDs_BIPs for 10%, 20% and 50% FBS in media. QDs_BIPs have shown stability over 4 hours time studies for percentage FBS in media. Overall QDs_MDP showed better dispersion and stability for all percentage of FBS containing media indicating minimal changes throughout the 4 hours time studies. Whilst QDs_EDP and QDs_IDP showed nearly 25% changed of absorbance values from initial fluorescence as increase percentage of media. All stabilised water soluble QDs_BIPs have shown good dispersion profile in aqueous solutions up to 50% FBS in media and also retained their fluorescent characteristics.

Several structurally different molecules and polymers have been suggested to modify the surface of quantum dots to provide improved biocompatibility and hydrophilicity [7, 26, 36]. The ligand exchange reactions used for EDP, MDP and IDP were designed based on well-documented phase transfer reported studies [33, 37, 38]. After the ligand exchange reactions, the QDs were characterised for their photoluminescence and size (TEM), and the efficiency of the ligand exchange reaction was monitored. Fluorescence spectroscopy of the modified QDs showed a decrease in photoluminescence; however this also indicated successful phase transfer resulting in biocompatible/water soluble quantum dots (Figure 3). TEM indicated that the QDs kept their size characteristics while ^{31}P-{^{1}H} NMR showed that ligand exchange was successful and no traces of TOPO or TOP could be found on the surface of the QDs [39]. BIP_QDs were also characterised for their zeta

potential and this was found to be within the range -0.50 mV to 0.05 mV for all BIP_QDs (~pH 7.0 at room temperature). The neutral readings (-10 mV to +10 mV) indicated that the nanoparticles were well dispersed in water and were suitable for further cell studies without cationic charge related cytotoxicity.

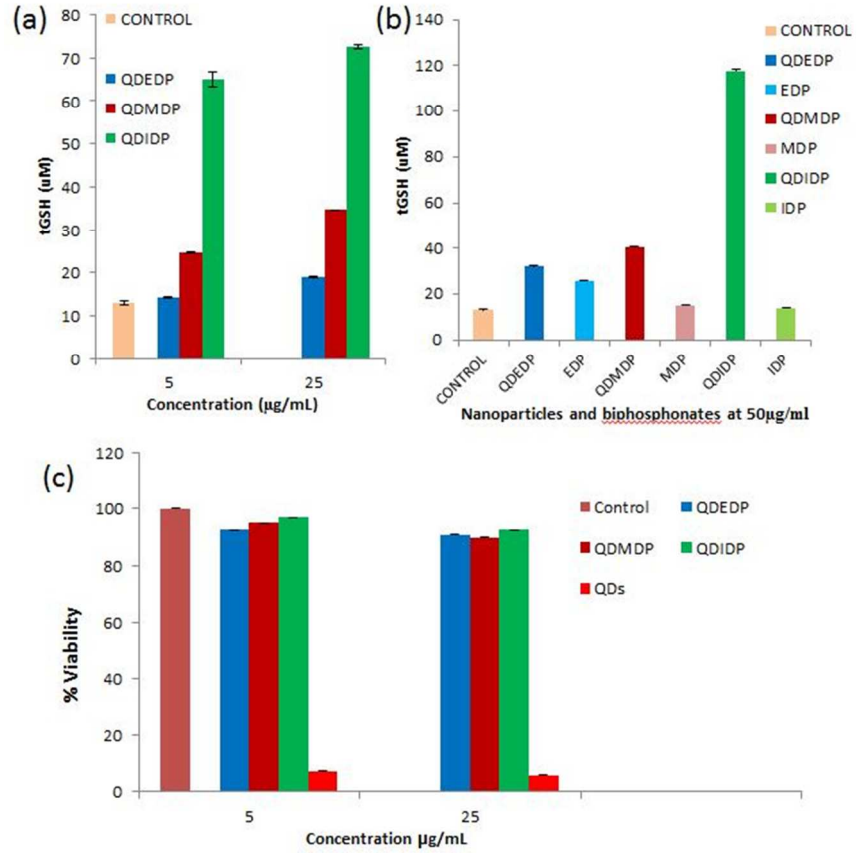

Figure 6: Cytotoxicity Studies of QDs_BIPs MTT and Glutathione Assay to measure cell proliferation. (a, b) Glutathione Assay to measure Reactive Oxygen Species (ROS) in IGROV-1 cells line for BIPs alone (EDP/MDP/IDP) and QDs_BIPs (c) MTT Assay QDs_BIPs and QDs_TOPO where QDs_TOPO show acute cytotoxicity on IGROV-1 cells. IGROV-1 cell toxicity studies exhibited a dose-response relationship on cell viability induced by the water soluble QDs_BIPs.

The photostability of the modified quantum dots in water was investigated as well as in aqueous solution with different pH values. The results (Figure 4) indicate the photostability of BIPs-coated QDs after repeated irradiation and show that 80% - 85% of the fluorescence intensity remains after 120 scans. Fluorescence intensity also remains unchanged at different pH values (Figure 4). This is important for bioimaging as QDs may diffuse through cell compartments with different pH values and therefore, their initial photoluminescence might be affected. It has been reported that low pH values can induce dissociation of thiolate ligands from cadmium

chalcogonide nanocrystals with an effect on their photoluminescence [40]. Studies have also shown that the photostability of surface-modified QDs is negatively affected after ligand exchange [41]. In our studies, BIPs-modified QDs show minimum change of photoluminescence at different pH values.

The QDs_BIPs also show good colloidal stability over time in media containing foetal bovine serum (FBS). We measured the effect of QDs_BIPs on the transparency of serum containing solutions as an assessment of the stability of the QDs_BIPs in biological systems. Colloidal stability studies were carried out with media 10%, 20% and 50% FBS. QDs_BIPs display minimum aggregation in aqueous media with or without serum over 4 hours in contrast to QDs_TOPO that do not disperse in aqueous media. QDs_EDP and QDs_MDP (non-nitrogenous) exhibited excellent colloidal stability in serum-containing biological media. The findings suggest that these water soluble quantum dots retain their colloidal stability required for application in cell imaging. QDs_IDP and QDs_EDP were slightly more turbid at higher serum concentration (Figure 5) than QDs_MDP, thus indicating the structure of the bisphophonate ligand has an effect on the colloidal stability of quantum dots. Stabilised bisphosphonate-capped quantum dots have shown good dispersion profile in aqueous solutions and retained their fluorescent characteristics [26].

There is concern over the potential toxicity of QDs containing cadmium within the core of the nanoparticles. The potential cytotoxicity of the semiconductor nanoparticles still remains unclear. Studies have been carried out investigating cell viability to determine the level of toxicity or exposure limits of these quantum dots [17, 42]. QDs_TOPO and QDs_BIPs underwent MTT assays to measure their effect on cell viability after 4 hours incubation whereas the effect on reactive oxygen species was assessed using the gluthathione assay. Figure 6c shows that QDs_BIPs induced a minimal effect on cell viability whereas QDs_TOPO caused significant cytotoxicity at both low and high concentrations. These data can be expected due to rapid cell uptake and leakage of the heavy metals into the cells [43]. Excellent viability with QDs_BIPs is observed even at the higher doses tested. This suggests that capping with bisphosphonates ligands has produced water soluble quantum dots with minimal effect on cell viability.

Determination of Cd^{2+} leakage induced reactive oxygen species (ROS) was carried out through glutathione assays using IGROV-1 cell lines. The QDs_EDP/MDP induces a small and dose dependent increase of intracellular total level of glutathione and in particular, QDs_EDP induces the minimum increase of total glutathione (non-significant difference to non-treated cells at 5 $\mu g\ mL^{-1}$). QDs_IDP show a significant increase of total glutathione for both concentrations compared to the other QDs_BIPs (EDP and MDP). This may indicate that IDP-coated QDs have inferior stability thus leading to intracellular Cd^{2+} leakage. Even at the lowest concentrations (5 $\mu g\ mL^{-1}$) QDs_IDP show elevated levels of total glutathione relative to untreated cells (control) and exhibit the highest total induced glutathione. We also measured the total glutathione levels induced by the BIP molecules (i.e. EDP, MDP and IDP) and their contributions towards the overall levels of total glutathione produced in the cells. Figure 6b shows that; BIPs do not affect the intracellular glutathione levels even at high concentrations (higher concentrations compared to the amount capping the QDs). It is possible that the release of Cd^{2+} ions intracellularly by the QDs_IDP is the main factor that contributes to cell impairment, cell death or the formation of reactive oxygen species as the effect of

bisphosphonates is minimal (Figure 6b).

Reported studies carried out with mercaptopropionic acid-coated cadmium telluride (CdTe) by Maysinger *et al.* showed that unmodified or 'naked' core CdTe can induce formation of reactive oxygen species (ROS) leading to multiple organelle damage and cell death. They also showed in the same study that effects associated with ROS formation can be prevented either with antioxidants treatment i.e. N-acetylcysteine (NAC-cysteine) or by further surface modification [44]. Niemeyer *et al.* have carried out systematic investigation on the generation of free radicals in aqueous solution by photoirradiation of stabilised CdS, CdSe and CdSe/ZnS with mercaptoacetic acid (MAA) through two methods (EPR spectroscopy and highly sensitive, radical-specific fluorimetric assays to measure generated radical species).

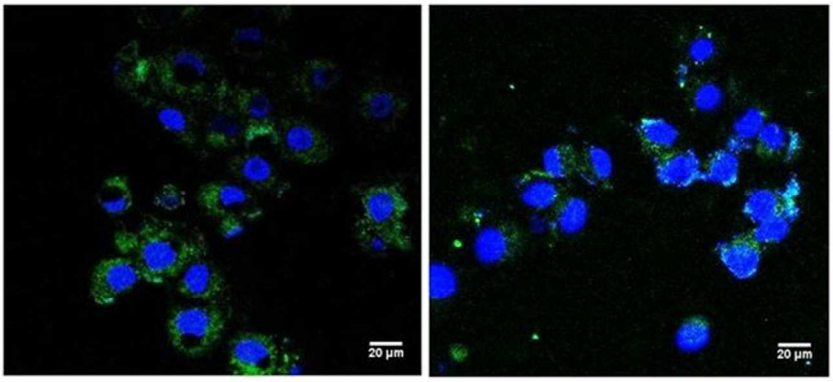

Figure 7: Confocal microscopy cell images of IGROV-1 cells labelled with DAPI (blue) and QDs_BIPs (green); QDs_EDP (right) and QDs_MDP (left). Imaging cells treated with QDs_IDP showed no fluorescent signal related to the QDs.

CdS generated both hydroxyl and superoxide free radicals whilst CdSe generated only hydroxyl free radicals which is in contrast with CdSe/ZnS that did not induce formation of free radicals under the condition used in the study [45]. Over-coating of a ZnS shell prevents the production of both free radicals with the higher-band-gap energy barriers as compared to core CdSe only [46]. Finally, Green and Howman *et al.* have reported generations of free radicals from QDs CdSe and CdSe/ZnS that are likely responsible for DNA nicking, both when incubated in the dark and exposed to the UV irradiation [47].

Many studies have been carried out to determine the level of toxicity i.e. investigating levels of QDs concentrations, exposure times of the nanoparticles, different cell types and also different surface coatings. From some of these studies, it has been clearly indicated that bare core QDs (either CdSe or CdTe); to have the most effect on cell viability [48]. QDs capped with another layer or multilayer of wider band gap ZnS or ZnSe, feature good capping material that contributes to the nanoparticles having longer exposure times in living cells and showing less toxicity, compared to naked core CdSe or CdS [49, 50]. Moreover, it has also been demonstrated that by going through surface modifications either through ligand exchange or encapsulation in liposomes or micelles the biocompatibility of the nanoparticles for

in vitro and *in vivo* experiments is greatly improved.

In order to assess the intracellular uptake of the nanoparticles, fluorescence microscopy experiments were carried out. IGROV-1 cells were co-incubated with QDs_BIPs at 50 μg mL^{-1} for 4 hours. Fluorescence microscopy images indicated significant intercellular quantum dots uptake. Images in Figure 7 show evidence that the nanoparticles are taken up by the cells. The amount of endocytosed QDs is sufficient to allow diffusion into the cellular cytoplasm. Together with the nuclear counter staining using DAPI, it can be seen that the nanoparticles QDs_MDP are found around the nucleus while the QDs_EDP label the cytosol. In contrast QDs_IDP showed minimum labelling of the cells supporting the hypothesis that IDP is a poor capping agent that allows QDs degradation in biological environments.

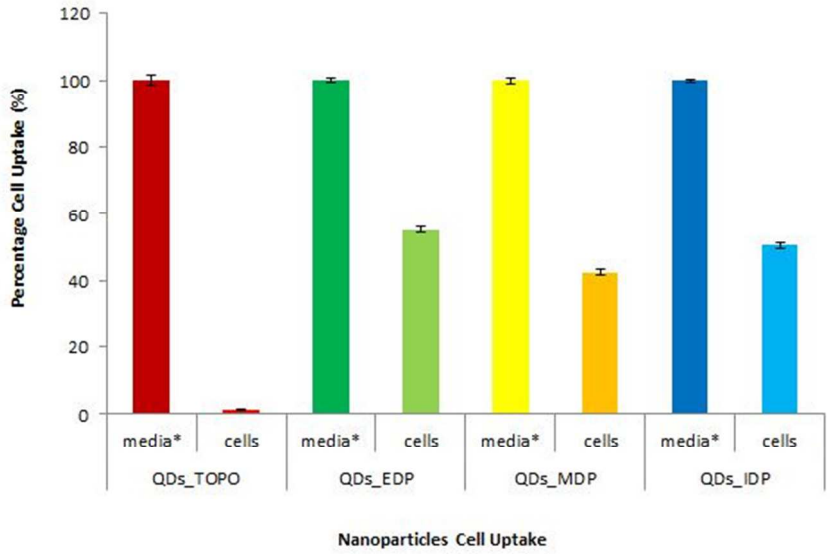

Figure 8: Intracellular uptake of QDs_BIPs measured through Inductive Coupled Plasma Mass Spectroscopy (ICP-MS). Intracellular Cd^{2+} cell measurements of QDs_TOPO and QDs_BIPs treated cells (24 hours incubation time; IGROV-1 cell lines). *media labelled in graph referring to media solution containing the nanoparticles at the same concentration used for cell uptake.

Data of cell uptake by Inductively Coupled Plasma Mass Spectrometry (ICP-MS) in Figure 8 indicated at least up to 60% of the applied QDs were taken up by the cells during 24 hours incubation studies, whilst there were minimal levels of Cd^{2+} of QDs_TOPO treated cells (less than 5% uptake) due to rapid cell death (cells were lysed and therefore most Cd^{2+} was in the cell lysate). The stabilised or as-prepared QDs_IDP have shown high cellular levels of Cd^{2+} even with relative colloidal aggregation (that would prevent their cell uptake). It is possible that out of the three BIPs studied IDP has weak or limited capping interaction between the BIPs/IDP with the surface of QDs and this phenomena leads to a shedding off of the QDs layer leading to cell damage. These findings correlated with the lack of imaging in cell labelling experiments where no labelling or fluorescence signals were observed

under confocal microscopy on QDs_IDP treated cells. There is also evidence that suggests that aggregation formed in the QDs_BIPs/IDP system can trigger the Cd^{2+} release due to the shedding of the capping layer and generation of Cd^{2+} ions into the biological solution that can contribute to the loss of fluorescence intensity.

4 Conclusions

Hydrophilic BIPs ligands offer an attractive route to produce biocompatible and water soluble quantum dots. Here we show that bisphosphonates have successfully produced water-soluble quantum dots that are colloidally stable in biological media even up to 50% serum. These QDs_BIPs are photostable and their fluorescence is pH independent and therefore can be used for cell imaging. The structure of the bisphosphonate appears critical for their colloidal and chemical stability. MDP and EDP modified QDs had minimal effect on cell viability and they show adequate cell internalisation and labelling of cells. Capping QDs with bisphosphonate ligands lead to colloidally stable fluorescent particles that can be used in bioimaging without compromising cell viability. In this study we have used the most widely explored QDs (CdSe/ZnS), and we hypothesise that selected non-nitrogenous bisphosphonates can act as biofunctionalisation agents on a wide range of imaging nanoparticles that require colloidal stability for imaging cells and tissues *in vivo*.

Acknowledgements

We acknowledge Dr Gema Vizcay-Barrena and Prof. Alice Warley, Centre for Ultrastructural Imaging in KCL, for TEM assistance; Mr Andrew Cakebread and Mr. Tobias Krams, Mass Spectrometry Facility in KCL, for Mass Spectrometry Analysis and Dr Jan Soetaert, Nikon Imaging Centre in KCL, for the kind training and guidance of the Microscopy Imaging (Confocal Microscopy). We gratefully acknowledge EPSRC (Theranostic Nanoparticles) and the Ministry of Science and Technology (MOSTI), Malaysia and the University Science Malaysia (USM) for the support and funding.

[1] *Institute of Pharmaceutical Sciences*
Franklin-Wilkins Building, KCL
150 Stamford Street
London, SE1 9NH
* maya.thanou@kcl.ac.uk

[2] *Department of Chemistry,*
Faculty of Natural Sciences, ICL
Exhibition Road,
South Kensington,
London SW7 2AZ

[3] *Departments of Physics,*
Strand Campus, KCL
London, WC2R 2LS

†*Electronic Supplementary Information (ESI) available: [**Schematic of the reaction and Mass Spectrometry Spectrum (GCMS) of ethylene diphosphonate (EDP)**]. See DOI: 10.1039/b000000x/*

References

1. A. P. Alivisatos, W. Gu and C. Larabell, *Annual review of biomedical engineering*, 2005, **7**, 55-76.
2. W. C. Chan and S. Nie, *Science*, 1998, **281**, 2016-2018.
3. M. A. Hines and P. Guyot-Sionnest, *J Phys Chem-Us*, 1996, **100**, 468-471.
4. N. Erathodiyil and J. Y. Ying, *Accounts of chemical research*, 2011, **44**, 925-935.
5. K. T. Yong, W. C. Law, I. Roy, Z. Ling, H. J. Huang, M. T. Swihart and P. N. Prasad, *J Biophotonics*, 2011, **4**, 9-20.
6. R. E. Bailey, A. M. Smith and S. M. Nie, *Physica E*, 2004, **25**, 1-12.
7. M. Geszke-Moritz and M. Moritz, *Mat Sci Eng C-Mater*, 2013, **33**, 1008-1021.
8. E. E. Lees, M. J. Gunzburg, T. L. Nguyen, G. J. Howlett, J. Rothacker, E. C. Nice, A. H. A. Clayton and P. Mulvaney, *Nano letters*, 2008, **8**, 2883-2890.
9. D. Gerion, F. Pinaud, S. C. Williams, W. J. Parak, D. Zanchet, S. Weiss and A. P. Alivisatos, *Journal of Physical Chemistry B*, 2001, **105**, 8861-8871.
10. B. C. Lagerholm, M. M. Wang, L. A. Ernst, D. H. Ly, H. J. Liu, M. P. Bruchez and A. S. Waggoner, *Nano letters*, 2004, **4**, 2019-2022.
11. E. R. Goldman, E. D. Balighian, H. Mattoussi, M. K. Kuno, J. M. Mauro, P. T. Tran and G. P. Anderson, *Journal of the American Chemical Society*, 2002, **124**, 6378-6382.
12. B. Dubertret, P. Skourides, D. J. Norris, V. Noireaux, A. H. Brivanlou and A. Libchaber, *Science*, 2002, **298**, 1759-1762.
13. F. Pinaud, D. King, H. P. Moore and S. Weiss, *Journal of the American Chemical Society*, 2004, **126**, 6115-6123.
14. A. M. Derfus, W. C. W. Chan and S. N. Bhatia, *Nano letters*, 2004, **4**, 11-18.
15. W. W. Yu, E. Chang, R. Drezek and V. L. Colvin, *Biochemical and biophysical research communications*, 2006, **348**, 781-786.
16. A. Hoshino, K. Fujioka, T. Oku, M. Suga, Y. F. Sasaki, T. Ohta, M. Yasuhara, K. Suzuki and K. Yamamoto, *Nano letters*, 2004, **4**, 2163-2169.
17. A. Shiohara, A. Hoshino, K. Hanaki, K. Suzuki and K. Yamamoto, *Microbiol Immunol*, 2004, **48**, 669-675.
18. J. Lovric, S. J. Cho, F. M. Winnik and D. Maysinger, *Chemistry & biology*, 2005, **12**, 1227-1234.
19. J. M. Tsay and X. Michalet, *Chemistry & biology*, 2005, **12**, 1159-1161.
20. Y. Zhang and A. Clapp, *Sensors (Basel)*, 2011, **11**, 11036-11055.
21. M. Xie, H. H. Liu, P. Chen, Z. L. Zhang, X. H. Wang, Z. X. Xie, Y. M. Du, B. Q. Pan and D. W. Pang, *Chemical communications*, 2005, 5518-5520.
22. I. L. Medintz, H. T. Uyeda, E. R. Goldman and H. Mattoussi, *Nature materials*, 2005, **4**, 435-446.
23. M. Gnant, *Cancer Treat Rev*, 2014, **40**, 476-484.
24. F. H. Ebetino, A. M. L. Hogan, S. T. Sun, M. K. Tsoumpra, X. C. Duan, J. T. Triffitt, A. A. Kwaasi, J. E. Dunford, B. L. Barnett, U. Oppermann, M. W. Lundy, A. Boyde, B. A. Kashemirov, C. E. McKenna and R. G. G. Russell, *Bone*, 2011, **49**, 20-33.
25. M. Grabolle, M. Spieles, V. Lesnyak, N. Gaponik, A. Eychmüller and U. Resch-Genger, *Analytical chemistry*, 2009, **81**, 6285-6294.
26. F. Dubois, B. Mahler, B. Dubertret, E. Doris and C. Mioskowski, *Journal of the American Chemical Society*, 2007, **129**, 482-483.
27. C. B. Murray, D. J. Norris and M. G. Bawendi, *Journal of the American Chemical Society*, 1993, **115**, 8706-8715.
28. Z. A. Peng and X. Peng, *Journal of the American Chemical Society*, 2002, **124**, 3343-3353.
29. B. O. Dabbousi, J. Rodriguez-Viejo, F. V. Mikulec, J. R. Heine, H. Mattoussi, R. Ober, K. F. Jensen and M. G. Bawendi, *The Journal of Physical Chemistry B*, 1997, **101**, 9463-9475.
30. M. J. Murcia, D. L. Shaw, H. Woodruff, C. A. Naumann, B. A. Young and E. C. Long, *Chem Mater*, 2006, **18**, 2219-2225.
31. M. Green, P. Rahman and D. Smyth-Boyle, *Chemical communications*, 2007, 574-576.
32. V. Biju, *Chemical Society reviews*, 2014, **43**, 744-764.
33. M. Green, *J Mater Chem*, 2010, **20**, 5797-5809.
34. M. Green, D. Smith-Boyle, J. Harries and R. Taylor, *Chemical communications*, 2005, 4830-4832.
35. D. V. Talapin, I. Mekis, S. Gotzinger, A. Kornowski, O. Benson and H. Weller, *Journal of Physical Chemistry B*, 2004, **108**, 18826-18831.

36. A. F. Hezinger, J. Tessmar and A. Gopferich, *European journal of pharmaceutics and biopharmaceutics : official journal of Arbeitsgemeinschaft fur Pharmazeutische Verfahrenstechnik e.V*, 2008, **68**, 138-152.
37. B. K. Pong, B. L. Trout and J. Y. Lee, *Langmuir : the ACS journal of surfaces and colloids*, 2008, **24**, 5270-5276.
38. S. Kim and M. G. Bawendi, *Journal of the American Chemical Society*, 2003, **125**, 14652-14653.
39. J. Wang, J. Xu, M. D. Goodman, Y. Chen, M. Cai, J. Shinar and Z. Lin, *J Mater Chem*, 2008, **18**, 3270-3274.
40. J. Aldana, N. Lavelle, Y. J. Wang and X. G. Peng, *Journal of the American Chemical Society*, 2005, **127**, 2496-2504.
41. Q. F. Ma, J. Y. Chen, X. Wu, P. N. Wang, Y. Yue and N. Dai, *J Lumin*, 2011, **131**, 2267-2272.
42. M. P. Jain, A. O. Choi, K. D. Neibert and D. Maysinger, *Nanomedicine*, 2009, **4**, 277-290.
43. D. Maysinger, J. Lovric, A. Eisenberg and R. Savic, *European Journal of Pharmaceutics and Biopharmaceutics*, 2007, **65**, 270-281.
44. J. Lovrić, S. J. Cho, F. M. Winnik and D. Maysinger, *Chemistry & biology*, 2005, **12**, 1227-1234.
45. B. I. Ipe, M. Lehnig and C. M. Niemeyer, *Small*, 2005, **1**, 706-709.
46. X. Michalet, F. F. Pinaud, L. A. Bentolila, J. M. Tsay, S. Doose, J. J. Li, G. Sundaresan, A. M. Wu, S. S. Gambhir and S. Weiss, *Science*, 2005, **307**, 538-544.
47. M. Green and E. Howman, *Chemical communications*, 2005, 121-123.
48. J. Lovric, H. S. Bazzi, Y. Cuie, G. R. Fortin, F. M. Winnik and D. Maysinger, *J Mol Med (Berl)*, 2005, **83**, 377-385.
49. F. M. Winnik and D. Maysinger, *Accounts of chemical research*, 2013, **46**, 672-680.
50. C. Kirchner, T. Liedl, S. Kudera, T. Pellegrino, A. Munoz Javier, H. E. Gaub, S. Stolzle, N. Fertig and W. J. Parak, *Nano letters*, 2005, **5**, 331-338.